

State of the Urban Forest:

San Francisco Bay Area-

Progress Report

Jim Simpson, Greg McPherson, Chad Delany
Center for Urban Forest Research
USDA Forest Service, PSW Research Station
Davis, CA
June 20, 2005

Introduction

The nine county San Francisco Bay Area contains over 200 municipalities and approximately 6.7 million people. Rapid growth, especially in outlying areas, is accelerating air pollution, water, and energy demand problems. These problems urgently need solutions. Urban forestry is integral to land use planning, mitigating water shortages, conserving energy, improving air quality, enhancing public health programs, increasing land values and local tax bases, providing job training and employment opportunities, reducing costs of city services, and increasing public safety. The goal of this study is to describe the region's urban forest structure and quantify the value of ecosystem services it produces. This information will enhance our understanding of the relevance and extent that urban forests impact the environmental and economic health of Bay Area communities, and the potential return on investment in planning and management.

As increasing population drives urban growth, impervious surfaces increase the flow of contaminants into water bodies, air pollution increases from commuting traffic, and more energy is required to support new development. The urban forest works to mitigate these adverse effects associated with the built environment. Impervious surfaces increase runoff during storm events. Urban trees retain rainfall on their leaf surfaces and reduce stormwater runoff. The built environment absorbs and stores solar radiation, causing urban heat islands that accelerate ozone formation and increase the need for air conditioning. Urban tree canopy cover can play a significant role by reducing the heat island effect through shading and evapotranspirational cooling of the air. City trees absorb air pollutants and sequester atmospheric carbon dioxide. By shading parked cars

and asphalt concrete streets, trees reduce the release of evaporative hydrocarbons that are involved in ozone formation. Tree shade and air temperature reductions reduce the rate that street surfaces deteriorate and repaving costs. Additionally, urban trees increase property values. Although any single tree benefit may be small, the sum of benefits is significant when it comes to mitigating the environmental impacts that result from converting natural land cover to built environments.

Study Area

The study area is the San Francisco Bay Area in California, USA (figure 1). The 20,000 square kilometer area is defined by the nine counties that surround the bay, San Francisco, Marin, Sonoma, Napa, Solano, Contra Costa, Alameda, Santa Clara, and San Mateo. The area consists of rangeland, agricultural fields, urban and peri-urban environments, and forests along the coast and western side of the bay. This region also includes such unique features as salt ponds, mudflats, saltwater wetlands, and vernal pools.

From 1980 to 2000, the population in this area has increased by 30%, from 5.1 million to 6.7 million people (2003). There are over 200 cities within this region that range in size from less than a thousand to over 900,000. San Jose (900,000), San Francisco (775,000), and Oakland (412,000) are the largest cities in the area. All the cities surrounding the bay form a large, continuous, urbanized area.

Population growth since 2000 has occurred primarily on former farmland on the region's edge, with at least 165,000 workers now commuting to the Bay area each day (King 2005). Cities experiencing relatively rapid growth include Brentwood, whose

population has nearly doubled to 41,000 in the past four years, Dublin, Fairfield, and Santa Rosa.

Figure 2 shows the location of the study area. The light gray color in the Landsat 7 image from 06 September 2002 is the built environment. The majority of the urban environment surrounds the San Francisco Bay, with a secondary area of development east of the Oakland Hills, which includes Pleasanton and Walnut Creek, and a string of cities in valleys north of the bay, such as the Sonoma and Napa Valleys.



Figure 1. Location of the nine county San Francisco Bay study area (USGS 2003; CaSIL 2004).



Figure 2. Location of nine counties and major cities in the San Francisco Bay area (CaSIL 2004).

The actual study area for this project is slightly smaller than the nine county area because Landsat path 44 does not include the northwest corner of Sonoma County (figure 3). As a result, six cities are excluded from the initial analysis of urban forest canopy cover change. Cloverdale is the largest city excluded and has a population of 6,800 people. The study area was masked to only include the urban areas within the overall study area as defined by the 2000 Census.

Deliverables

This progress report is the first of four project deliverables, and describes historic change in urban forest canopy cover. The other deliverables listed below will be included in the final report, which is due March 1, 2006:

1. Historic canopy cover change for the nine county region (except northern Sonoma Co.) will be displayed based on Thematic Mapper (TM) data for 1984, 1995, 2002. Also, we will map change in impervious (rooftops, paving) and pervious (turf, bare soil) land cover for these periods. In the final report, tabular data will list our findings for each city and county.
2. The value of annual benefits produced by the current tree canopy will be mapped and listed for each city and county using higher resolution ASTER imagery. To derive estimates of resource units (e.g., kWh of electricity saved, tons of ozone uptake) and to monetize tree benefits, the region will be divided into 5 climate regions and three tree zones that correspond with our reference city data collected in San Francisco, Berkeley, and Modesto. Canopy will be stratified by land use (residential, non-residential developed, park developed, other, forest land) (table 3).
3. The value of future tree canopy will be determined assuming agreed upon land development, projected urban growth, tree planting, and conservation levels.
4. Benefit-cost tables for typical large, medium, and small trees will be produced as a reference for designers, planners, and managers. The 40-year stream of annual benefits and costs will be listed for each 5-year interval after planting. Examples

will show how to adjust these data to estimate benefits from proposed tree planting projects.

Project Status

The project is currently on schedule and will be completed by March 1, 2006. The historic canopy cover analysis has been completed and the benefit cost analysis for the West Bay has been partially completed as a proof of concept. Tasks and completion dates are shown in Table 1 and organized by project subsection in Figure 4

Table 1. Timeline for the Bay Area project.

Task	Time
Order TM Imagery	Completed
Orthorectify TM Imagery	Completed
Calibrate TM Imagery	Completed
Classify TM Imagery	Completed
Change Detection	Completed
Map Climate Regions	Completed
Map Land Use	Completed for West Bay.
Tree Species Distribution	Completed for West Bay
Tree Age Distribution	Completed for West Bay
Tree Cost Surveys	Completed
RU Data Sources	Completed
Progress Report	Completed
RU Data Collection	Completed for West Bay
Order & Orthorectify ASTER imagery	June 30, 2005
RUs, QA/QC	June 1 – August 31, 2005
Calibrate ASTER imagery	July 31, 2005
Classify ASTER imagery	August 31, 2005
Develop Benefit-Cost tables	August 31, 2005
ASTER current tree value	September 30, 2005
ASTER future tree value	October 31, 2005
GIS Work – County & City tables	November 30, 2005
Write draft report	December 31, 2005
Review / revise final report	January 31, 2006
Print / Distribute	February 28, 2006

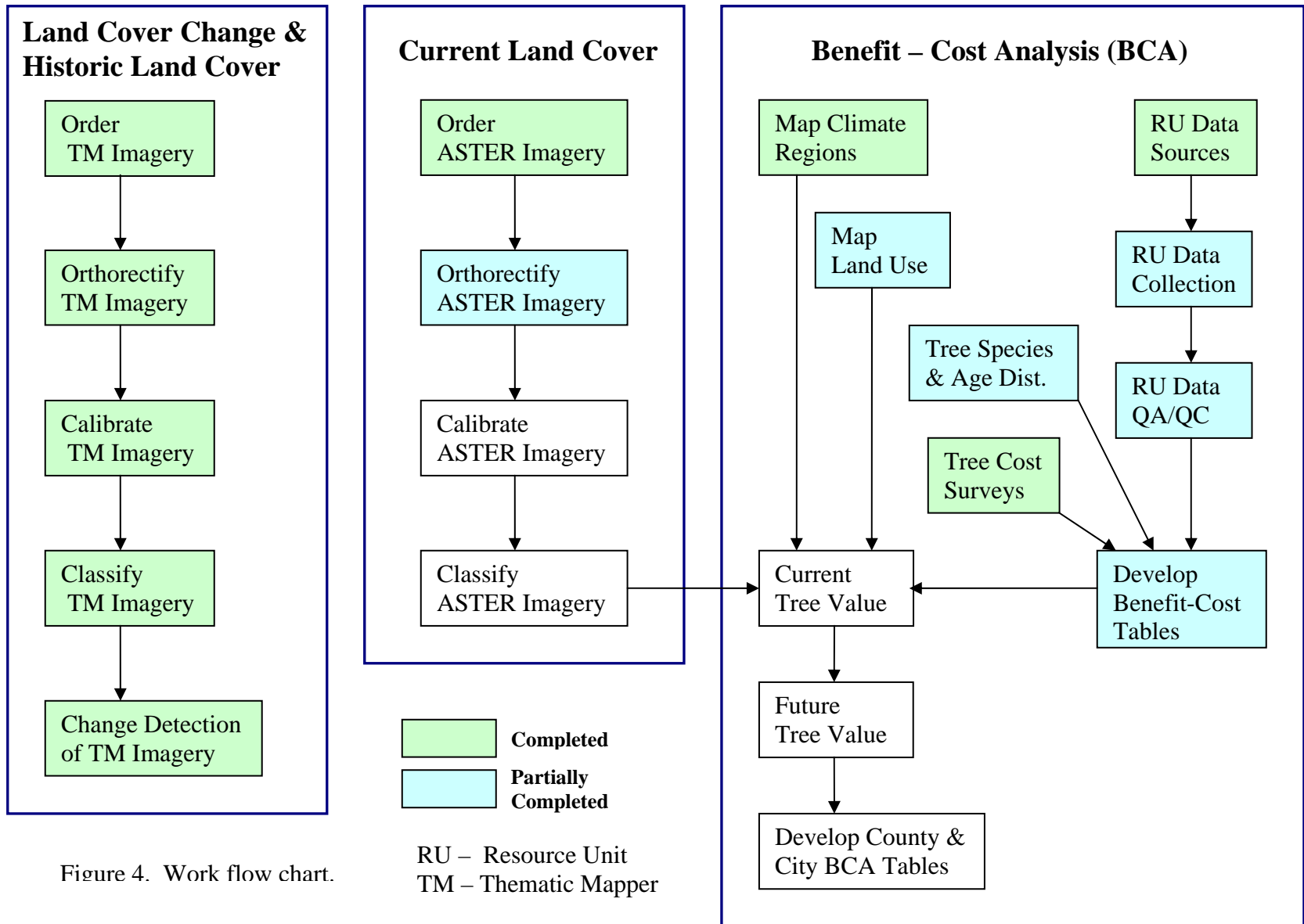


Figure 4. Work flow chart.

1. Canopy Cover Change 1984-2002

Introduction

Remote sensing provides an efficient method for characterizing the changes in the ecosystem as it is converted from a natural to built environment. Medium (~30 m) resolution satellites have been in operation for over twenty years. These datasets allow for the measurement of the size, distribution, and composition of the urban ecosystem as it has changed over this time period

Objects in urban environments have a characteristic scale of 10 – 20 m (Small 2003). At a spatial resolution of 30m, the satellite imagery is not able to consistently measure single objects. Initial remote sensing studies of urban land cover used traditional hard classifiers which assume a single class for each pixel. These classification techniques are not statistically valid in an urban environment where the majority of the pixels are a combination or mixture of classes.

Instead of assigning each pixel a land use type within the urban environment, Ridd (1995) characterized the urban ecosystem with the Vegetation-Impervious surface-Soil (V-I-S) model. In this model, the urban environment is defined as a combination of green vegetation, impervious surface, and soil. Water surfaces are ignored or masked out of the analysis.

Since urban environments are characterized by objects that are smaller than the spatial resolution of Landsat Thematic Mapper, the pixels are spectrally a mixture of the different objects covered by the pixel. To characterize the urban environment, sub-pixel estimates of urban land cover are needed. Spectral Mixture Analysis (SMA) has been very successful in studying urban environments. SMA gives a subpixel estimate of each

land cover defined by an endmember. Endmembers define the spectrally pure instance of each land cover. Variations of SMA have been used to characterize a variety of urban environments (Phinn *et al.* 2002; Wu *et al.* 2003; Small 2005).

Phinn *et al.* (2002) found linear spectral mixture analysis to be the most accurate method for determining the V-I-S model with moderate resolution satellite imagery. SMA has the advantage that each fraction is based on a physical and measurable quantity. Other transformation techniques such as Kauth-Thompson provide estimates of greenness, brightness, and wetness but are not directly tied to physically quantifiable materials such as vegetation, impervious surface, and soil (Small 2005).

The standard SMA model for urban classification uses four endmembers: vegetation, soil or non-photosynthetic vegetation (NPV), impervious surfaces, and shade (Wu *et al.* 2003; Wu 2004). The shade component of the model is problematic. The shade component in an urban environment measures actual shade caused by nearby buildings or water or a darker example of an endmember. Because of the shade component in the analysis, the endmembers chosen for vegetation, NPV, and impervious surfaces are bright examples of these surfaces. The actual subpixel area covered by one of these three physical endmembers is some combination of vegetation, NPV, or impervious surface plus the shade component. For example, if concrete were used as the impervious endmember then asphalt would be represented in this model as a combination of impervious surface and shade. The shade component is not actual shade but instead is only measuring how much darker the asphalt is than the concrete. In this example, part of the asphalt is misclassified as shade.

Although the shade component is problematic, it does contain important information that can be used to discriminate between irrigated grass and canopy cover. Roberts *et al.* (1999) used the shade and vegetation component to discriminate between agricultural fields and canopy cover in the Amazon rain forest. Since trees and shrubs shade themselves, canopy cover is characterized by a combination of vegetation and shade. Irrigated lawns and golf course fairways do not shade themselves and are therefore described by only a vegetation fraction.

Different approaches have been used to minimize the problem with shade. Wu & Murray (2003) estimated impervious surfaces by combining the impervious surface fraction with the shade fraction to determine the overall impervious surface fraction. Wu (2004) found that this technique worked only for fully urbanized environments but did not perform well in residential areas or at the wildland-urban interface. He suggested the use of a normalized spectral mixture analysis (nSMA) where brightness variations were reduced by using the mean value for all the bands. This preserved the shape of the spectral curve between the different endmembers but minimized the brightness variations. With the nSMA model, only three endmembers are used and shade is removed. This model produced better results over a wider range of urban and peri-urban environments.

Small (2002; Small 2004) used a different approach, a three endmember SMA model of vegetation, bright albedo, and dark albedo. He showed that the urban environment can be uniquely characterized from natural environments with this model. The defining characteristic of the urban environment is its spectral mixture. The majority of urban pixels are mixed and not pure examples of a specific land cover.

Methods

We measured historic canopy cover, canopy cover change, historic impervious surface extents, and its change with Thematic Mapper (TM) and Enhanced Thematic Mapper Plus (ETM+) imagery from 1984, 1995, and 2002 (table 2). The dates of the satellite imagery are nearly the same for each year and the solar elevation and angle are closely matched between the Thematic Mapper images. This produces shading conditions within the images that are comparable.

In order to produce reliable results, the satellite imagery was orthorectified and radiometrically calibrated. Aerial photography used for orthorectification and accuracy assessment was taken only a month after the ETM+ imagery (USGS 2004). This reduces temporal decorrelation between the 2002 ETM+ data and the aerial photography. This is especially important since certain areas were being developed during the one month period between when the satellite imagery and aerial photography were taken.

Orthorectification converts satellite imagery to a map (Jensen 1996). The process includes georeferencing an image to a map coordinate system and adjusting for parallax distortions caused by elevation changes. The ETM+ 2002 image was orthorectified to high-resolution natural-color orthorectified aerial photography. The 1984 and 1995 TM images were orthorectified to the 2002 ETM+ image. The standard orthorectification accuracy for TM and ETM+ imagery is 15m. We were able to achieve an accuracy of 7.5m for the 2002 image and 10.3m accuracy for the 1995 and 1984 images. One hundred and thirty points were sampled from throughout the area for the orthorectification. For a discussion of orthorectification accuracy see the ERDAS Field Guide (ERDAS 2002)

Table 2. Satellite imagery.

Imagery	Date	Resolution	Ortho Accuracy
TM	07 September 1984	30m	10.3 m
TM	06 September 1995	30m	10.3 m
ETM+	01 September 2002	30m	7.5 m
Aerial Photography	October 2002	0.6 m	6.2 m

Radiometric calibration corrects imagery for differences in sensor calibration and atmospheric conditions. The imagery was acquired during clear sky conditions but the calibration of the sensor drifts. The 2002 ETM+ imagery was converted to exoatmospheric reflectance based on published post-launch calibration coefficients (USGS 2005). Objects within the image that are considered radiometrically stable, such as deep lakes, were chosen as Pseudo-invariant (PIV) image endmembers. Golf course fairways, flat rangeland, and building rooftops were also used as PIVs. The 1995 and 1984 images were radiometrically calibrated with linear regression to the 2002 ETM+ image using the PIVs with an $R^2 = 0.99$.

Preliminary investigation of the imagery began with a Minimum Noise Fraction transformation (MNF). A MNF transformation is a cascading form of Principle Component Analysis. The MNF transformation orients the axes to include the signal to noise ratio for each of the bands. The statistics for the signal to noise ratio are derived from the imagery within a user defined homogenous area. By looking at the scatterplots between the first three components of the MNF, the overall shape of the spectral mixing space within the imagery is determined (figure 5).

An MNF transformation was also conducted on only the urban areas. Figure 6 illustrates how the feature space becomes less complex when only the urban areas within the study area are considered. The pixels that are at the vertices of the feature space

Figure 5. These scatterplots are a two dimensional projection of a three dimensional cloud of points that define the feature space. The color represents the point density. Yellow and green are the lowest point densities. Blue and cyan represent the highest density. They are between MNF components a. 1 and 3; b. 2 and 3; and c. 1 and 2. They show three alternate views of the same cloud of points. The regions at the edge or corners of the scatter are pure pixels of one land cover. The majority of the pixels are mixed and in the middle of the scatterplot. In order to describe an area with linear mixture modeling, it needs to have a triangular appearance with concave edges. When both the natural and urban environments are considered together, a three or four endmember linear mixture model is not adequate.

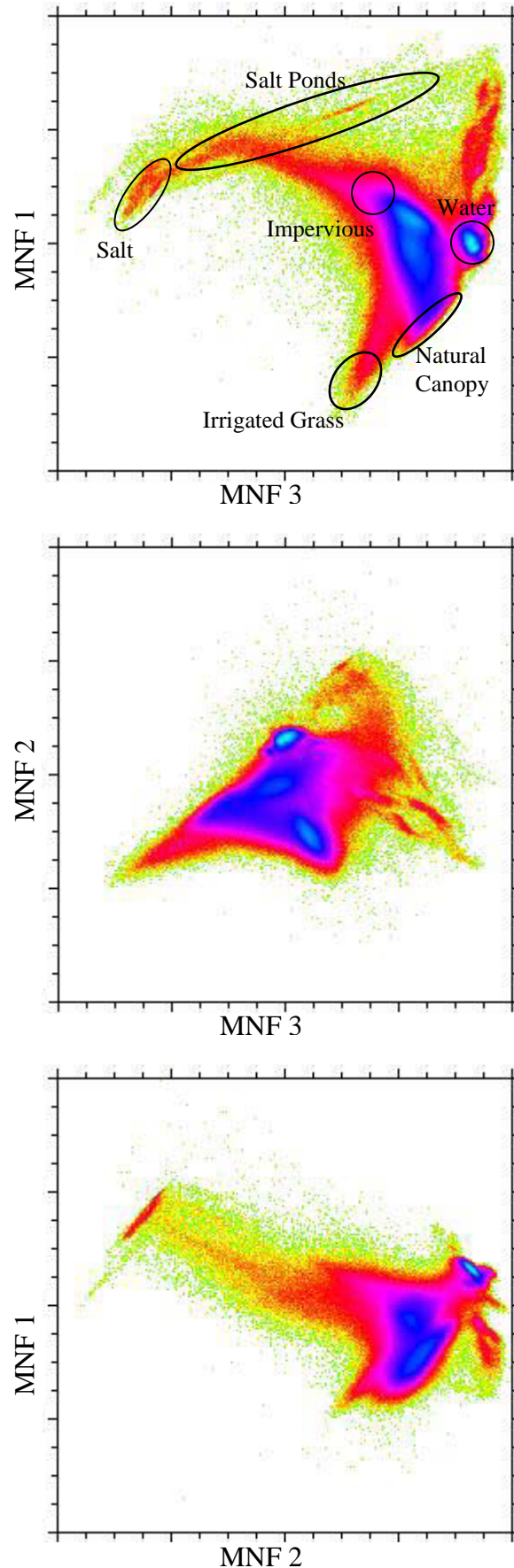
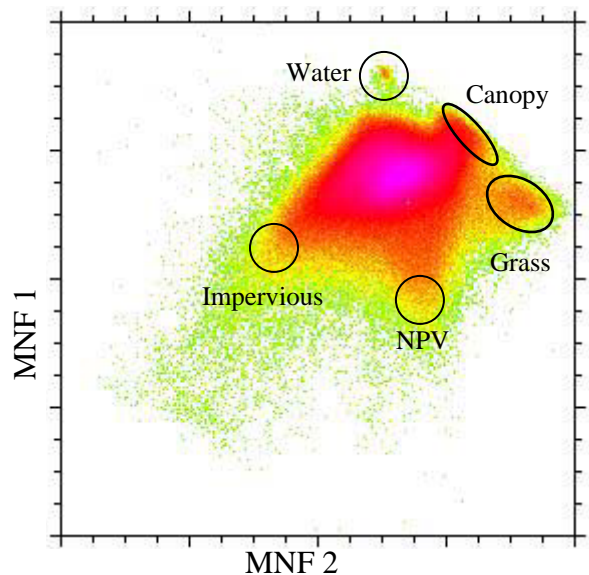
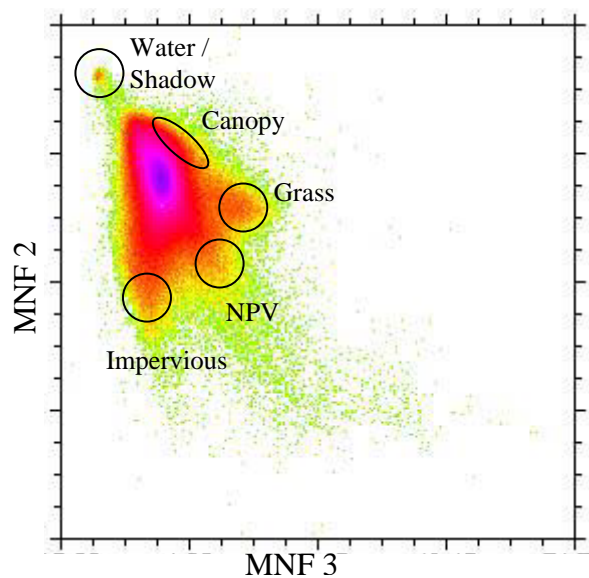
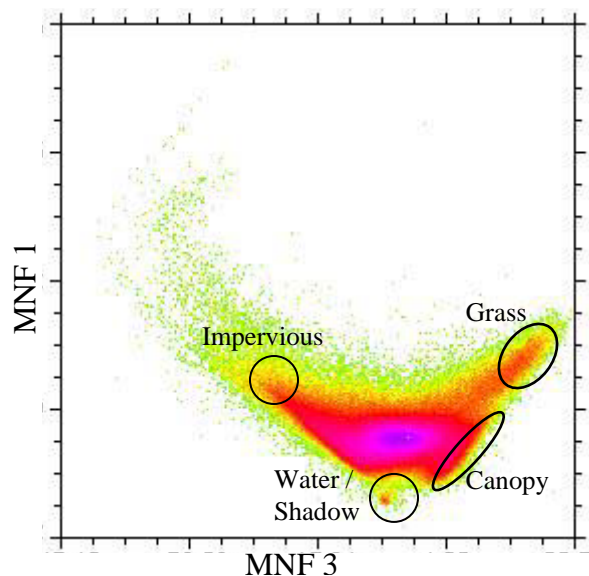


Figure 6. When the area is restricted to only the urban environment, the feature space does collapse to a triangular mixing space with concave edges. There is some non-linear mixing associated with the canopy cover as seen by the slightly convex edge between water or deep shadow and irrigated grass. In figure c., the NPV endmember becomes obvious.



represent pure or unmixed pixels. These pixels are candidates for endmembers used in the spectral mixture analysis. The simplified triangular mixing space of the urban areas shows that it can be modeled by linear spectral mixing with a minimum of three endmembers, although four endmembers is also possible.

In this study, we use the V-I-S model but modify the green vegetation component. In an urban environment, green vegetation is composed of trees, shrubs, and irrigated grass. We are interested in the canopy cover from trees and shrubs. We remove the irrigated grass portion from the green vegetation component to form a canopy cover category and add the irrigated grass to soil to form a pervious surface category. Our model of the urban environment changes Vegetation – Impervious Surface - Soil to Canopy Cover – Impervious Surface – Pervious Surface. Land cover under the tree canopy is not characterized.

In order to tease out a canopy cover sub-pixel estimate, we will use a combination of the nSMA variation and Small's SMA model to determine canopy cover. Impervious surfaces and soil / NPV will be characterized by the normalized SMA model. The two classifications will be combined to provide an overall canopy cover – impervious surface – pervious surface subpixel estimate for the San Francisco Bay Area.

Wu (Wu 2004) only tested the accuracy of the nSMA model for Columbus, Ohio and for only one land cover class: impervious surface. We will test the normalization method on the large and varied environment of the entire San Francisco Bay Area and calculate the accuracy for all three land cover components.

The nSMA model transforms the feature space . Using the standard Principle Component Analysis for the urban areas results in a linear mixing space defined by three

endmembers: impervious surfaces, NPV / soil, and vegetation (1999; 2000; ERDAS 2002; Wu 2004). The normalization method removed the shade component from the mixing space. This technique provides a more robust method for estimating the three endmembers throughout the urbanized Bay Area.

In order to discriminate canopy cover from irrigated grass within the vegetation fraction, we need to reintroduce the shade component. We followed the model proposed by Small (2002) that urban environments can be defined by three endmembers: vegetation, dark albedo, and bright albedo. This model performs well except for in areas that the unmodeled soil / NPV class predominates. The Small SMA model will only be used to discriminate canopy cover from irrigated grass within the vegetation fraction estimated by the normalized SMA method.

Gilbert *et al.*(2000) modeled reflectance from heterogeneous canopy cover and found that it is not governed by linear mixing. At the landscape scale for homogenous canopy cover, linear mixing is a feasible approximation. A more detailed spatial analysis of heterogeneous canopy cover highlights the non-linear mixing and shadowing that occurs within the canopy cover. For trees and shrubs that are dispersed and do not form a closed canopy, vegetation is systematically underestimated. This is caused by the significant shading component associated with dispersed plants. The aerial photography will be used to calibrate and correct for the systematic underestimate of the vegetation component and to assess the accuracy of the overall classification.

A number of areas were masked from the imagery before classification because of spectral confusion. The salt ponds are easily confused with bright impervious surfaces, such as light-colored rooftops. Because water and shade are spectrally similar, water

needs to be masked from the imagery before classification. Large areas of grass, such as parks and golf course fairways that produced spectrally pure pixels of unshaded vegetation were also removed by masks from the imagery. This reduces the confusion between irrigated grass and canopy cover within the vegetation fraction of the classification.

The water mask was constructed from portions of the National Wetlands Inventory and a Spectral Angle Mapper classification of water within each of the three images. Salt ponds and tidal salt marshes change dramatically in their spectral signature within the three Landsat images but do not change in their land cover extent. They were masked out based on the National Wetland Inventory. Open water, reservoirs, lakes, and streams were classified with the Spectral Angle Mapper. These classified areas of water did change in their extent throughout the imagery. The Spectral Angle Mapper performed well in classifying water with large sediment loads in the bay. Shadows caused by the large buildings in downtown San Francisco were confused with water in all classification methods attempted but had the least confusion with the Spectral Angle Mapper. Other shaded urban areas were not classified as water by the Spectral Angle Mapper. The water mask was hand edited to not include the downtown San Francisco area.

Urban areas have unique irrigated grass regions associated with specific land uses. These areas are large enough to produce spectrally pure regions of unshaded vegetation or grass. Since the imagery is from September, all grass that is not irrigated has turned brown. The only areas of unshaded green vegetation are irrigated grass areas in parks, golf course fairways, and agricultural fields, which are masked out as described above.

The areas of irrigated grass were identified with the Spectral Angle Mapper. The classification of the areas was modified by including contextual and texture information. Since the areas of interest produce sharp contrast with the surrounding environment and they form a contiguous conglomeration of pixels, information about the variance of red, near-infrared, and short-wave (TM bands 3, 4, and 5) and a neighborhood function were included in the classification of irrigated grass areas.

The aerial photography was sampled for calibration and accuracy assessment of the land cover classes: trees, impervious surface, and porous surface. There were a total of 650 points randomly sampled within four different regions of the study area: San Francisco, San Jose, Walnut Creek – Oakland Hills, and the area surrounding the San Antonio reservoir. Half of these points were used for calibration; the other half for accuracy assessment. Each sampled area was a 3 x 3 pixels or 90m x 90m area. The different land covers were digitized from natural color aerial photography. The sampled area was 90m x 90m in order to minimize the effects of errors in the georeferencing (Wu, 2004).

Accuracy is measured by Root-Mean-Squared Error (RMSE) and Systematic Error (SE)(Wu 2004). RMSE measures the overall accuracy for each of the 650 samples. SE measures how much the sample overestimates or underestimates the land cover. This error is the error associated with each individual pixel approximation of land cover (table 3). In the final report, error will also be estimated on an object or city-wide scale.

Table 3. Error associated with classification.

	RMSE	SE
Canopy Cover	13%	+3%
Impervious Surface	14%	-2%
Porous Surface	15%	-1%

Wu (2004) using the normalized SMA technique and only measuring impervious surface for Columbus, OH had an RMSE of 10.1% with an SE of -3.4%. Wu and Murray (2003) also only measuring impervious surface for Columbus, OH had an RMSE of 22.2% and an SE of 15.9%. Small (Small 2001) compared vegetation fractions (not canopy cover) from Thematic Mapper imagery with “illuminated vegetation” in high-spatial resolution imagery. He assumed a 10% error for each point and had an R^2 fit of 0.999.

The results of the analysis were presented by urban area as defined in the 2000 Census (U.S. Census Bureau 2002). This will show how land cover has changed from 1984 to 2002 for an area that is now considered urban. The overall percentage of canopy cover and impervious surface for each urban area will be reported for 1984, 1995, and 2002. The percentage of change in canopy cover and impervious surface for each urban area between 1984 and 2002 will also be discussed. Changes in canopy cover and impervious surface per pixel of greater or less than the RMSE and SE associated with each category were also mapped for the Study Area.

Besides quantifying land cover conversion from a natural to urban environment for an area that is currently urban, we also analyzed the growth pattern of the urban boundary from 1984 to 2002. Urban extent was calculated from the spectral mixture analysis. Pixels were classified as urban based on an impervious surface percentage greater than 20% within the study area (Lu *et al.* 2004). Large grass areas such as parks

and golf courses that had previously been masked were also added to the area classified as urban.

Results and Discussion

The population has increased 30% in the nine-county Bay Area from 1980 to 2000 (ABAG 2003). During that time, the urban built environment has increased 73%, from 1,620 square kilometers (625 square miles) to 2,800 square kilometers (1,080 square miles). Overall urban area increased from 8% to 14% of the total landcover. This conversion of landcover is associated with an increase of impervious surfaces and canopy cover since urban areas have more trees than the surrounding natural area.

Using the current urban area boundaries as defined by the 2000 Census for analysis, we studied how land cover has changed with urbanization from 1984 to 2002. Canopy cover has increased within this area by 10% and impervious surfaces have increased by 17% (table 4). Urban expansion has been primarily into rangeland and agricultural areas. This has had the affect of increasing canopy cover but the increase in canopy cover has not kept pace with the increase in impervious surfaces. The increase in impervious surfaces between 1984 and 1995 was almost double that of canopy cover.

Table 4. Landcover conversion within current urban area boundaries.

	1984	1995	2002	Per-Pixel RMSE	Object RMSE
Canopy Cover	19%	25%	29%	13%	To Be Determined
Impervious Surface	39%	50%	56%	14%	To Be Determined
Pervious Surface	42%	25%	15%	15%	To Be Determined

Figures 7 – 9 show the spatial distribution of canopy for each urban area for 1984, 1995, and 2002. The change in canopy cover from 1984 to 2002 is in figure 10. Figures 11 – 13 show the spatial distribution of impervious surface for each urban area for 1984, 1995, and 2002. The change in impervious surface from 1984 to 2002 is in figure 14.

The established urban areas of San Francisco and Oakland do not greatly change during this twenty year period. The majority of the increase is in San Jose and then urban areas around the bay, the area east of the Oakland Hills, and the cities region north of the Bay including the Sonoma and Napa valleys.

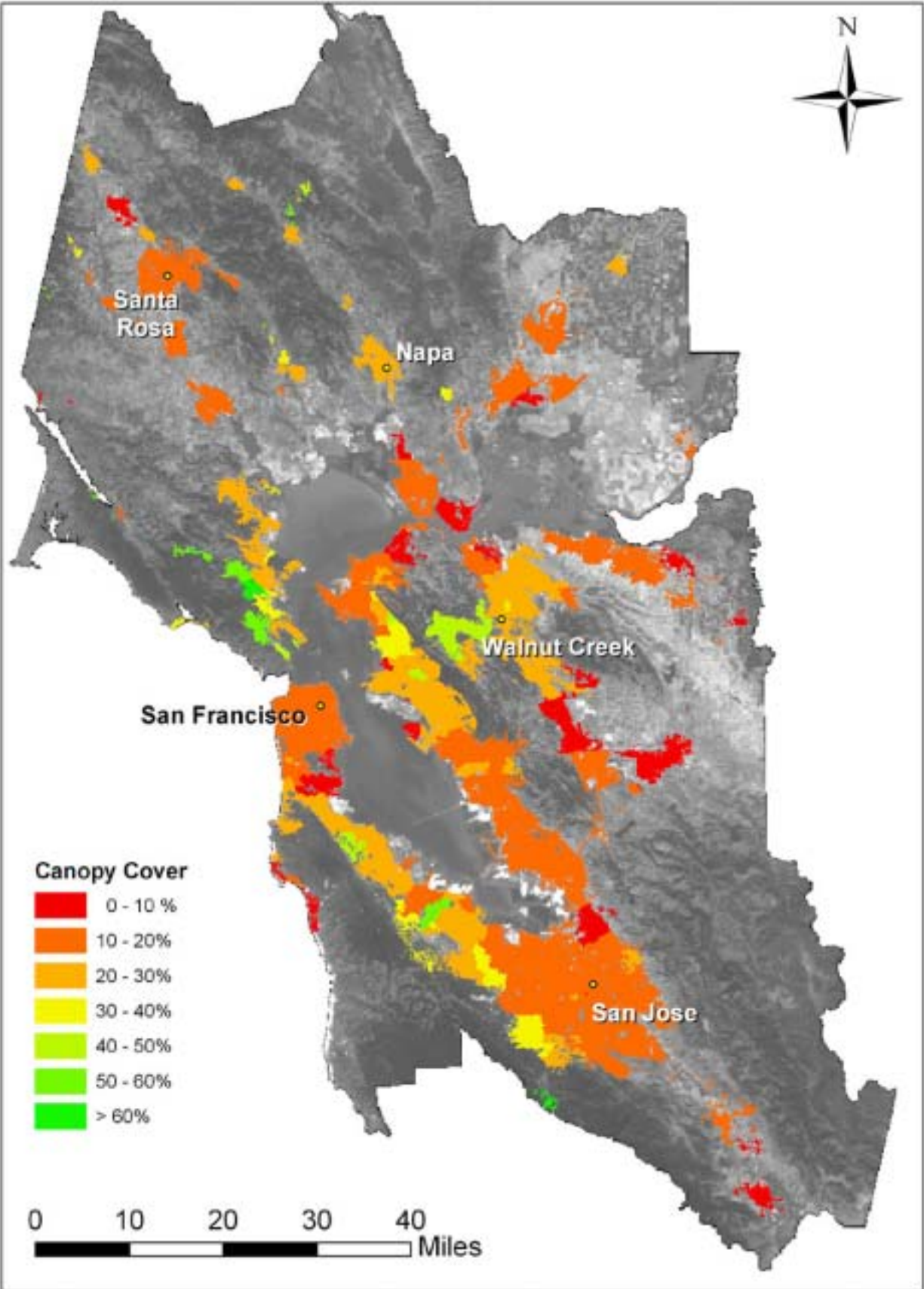


Figure 7. 1984 canopy cover percentage for each of the urban areas within the study area.

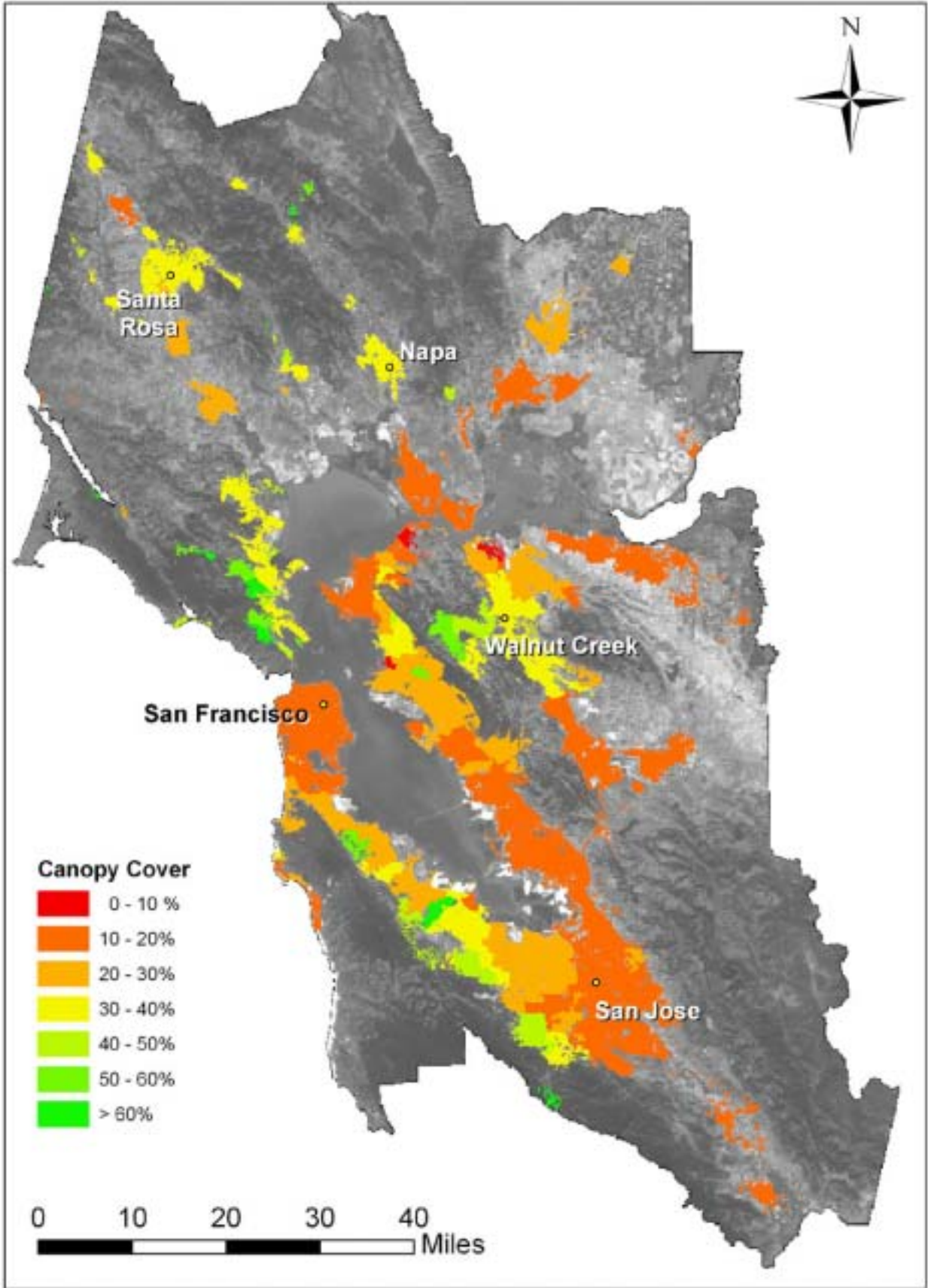


Figure 8. 1995 canopy cover percentage for each of the urban areas within the study area.

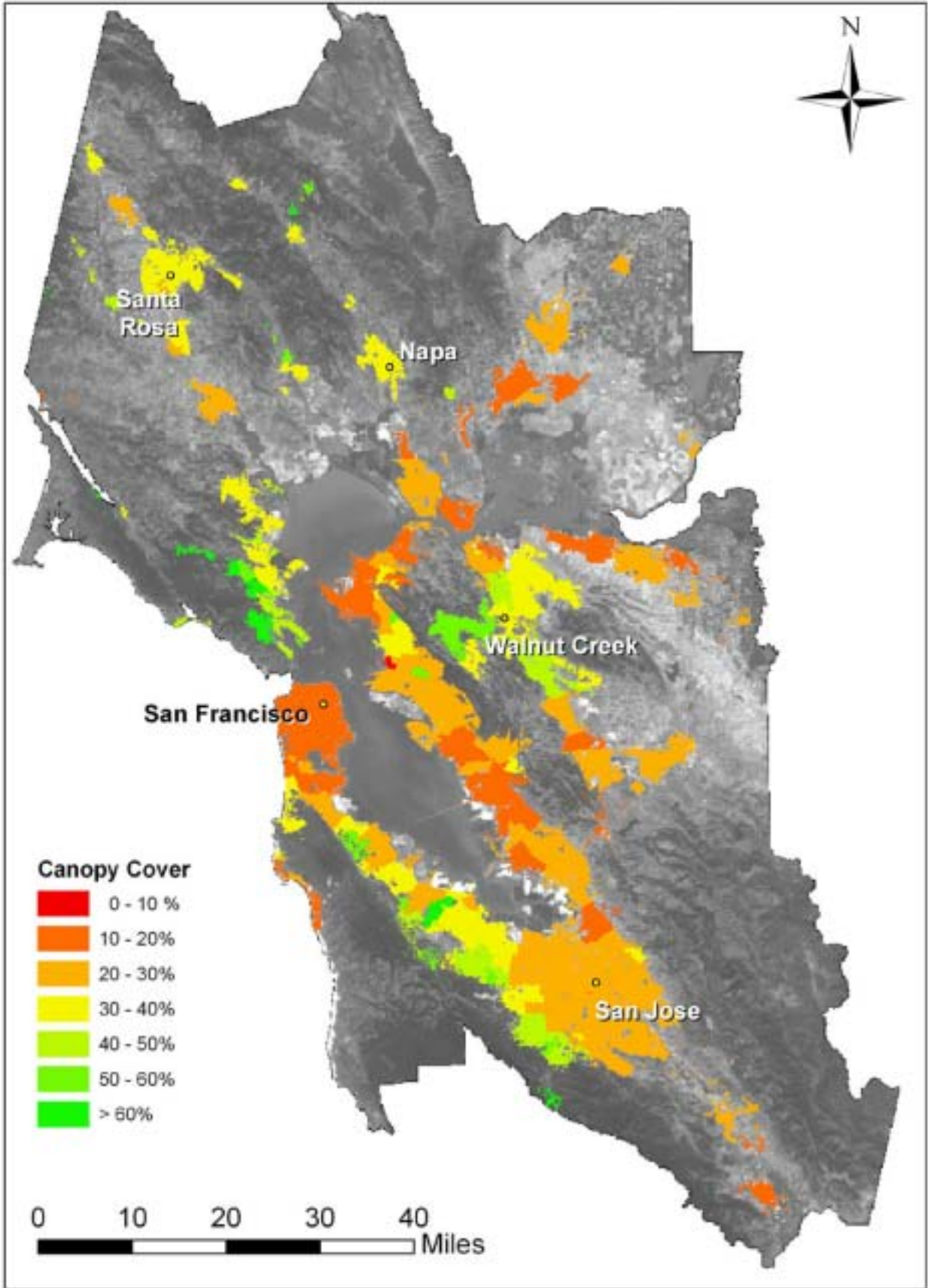


Figure 9. 2002 canopy cover percentage for each of the urban areas within the study area.

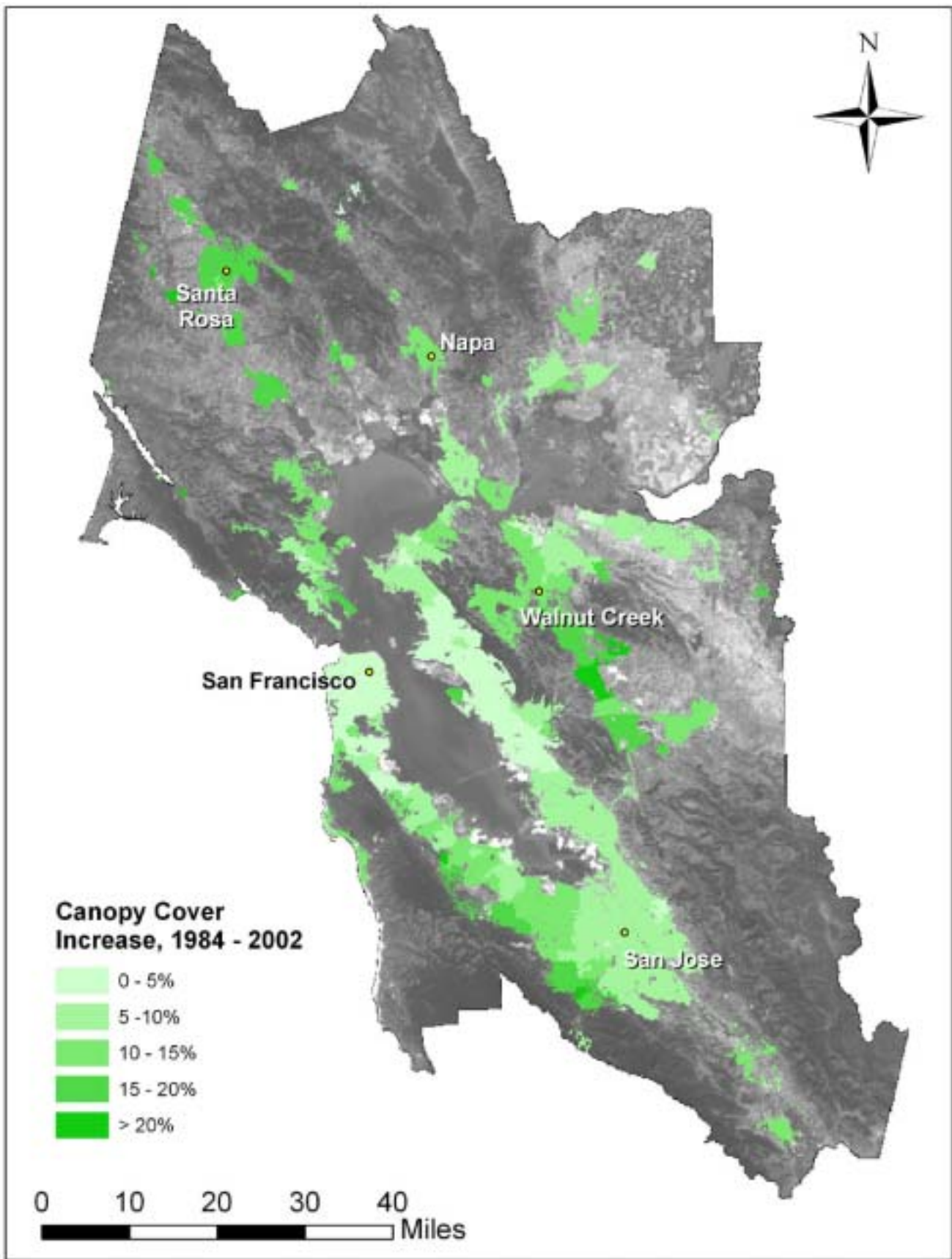


Figure 10. Canopy cover increase from 1984 to 2002 per urbanized area.

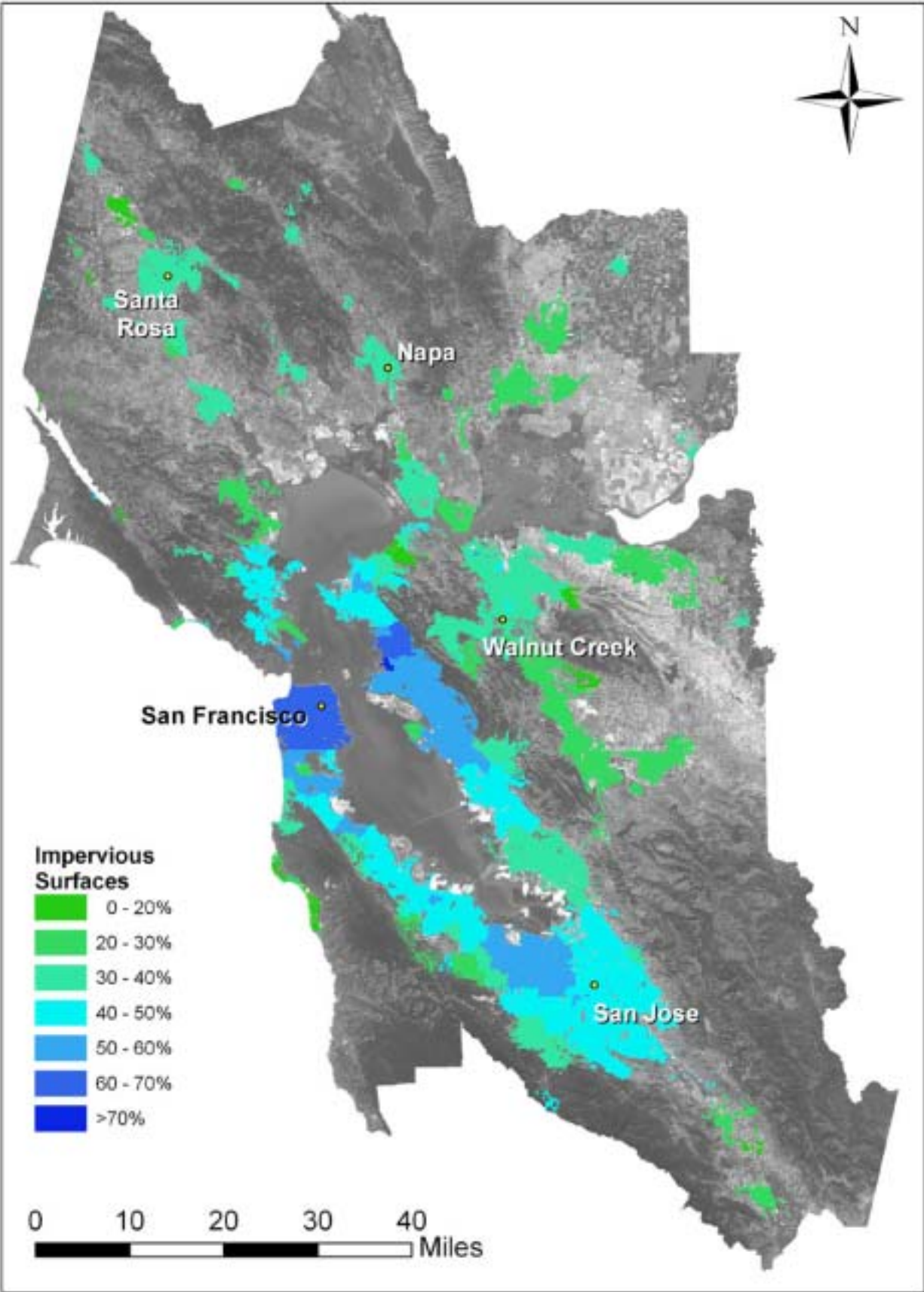


Figure 11. 1984 impervious surface extent for each of the urban areas within the study area.

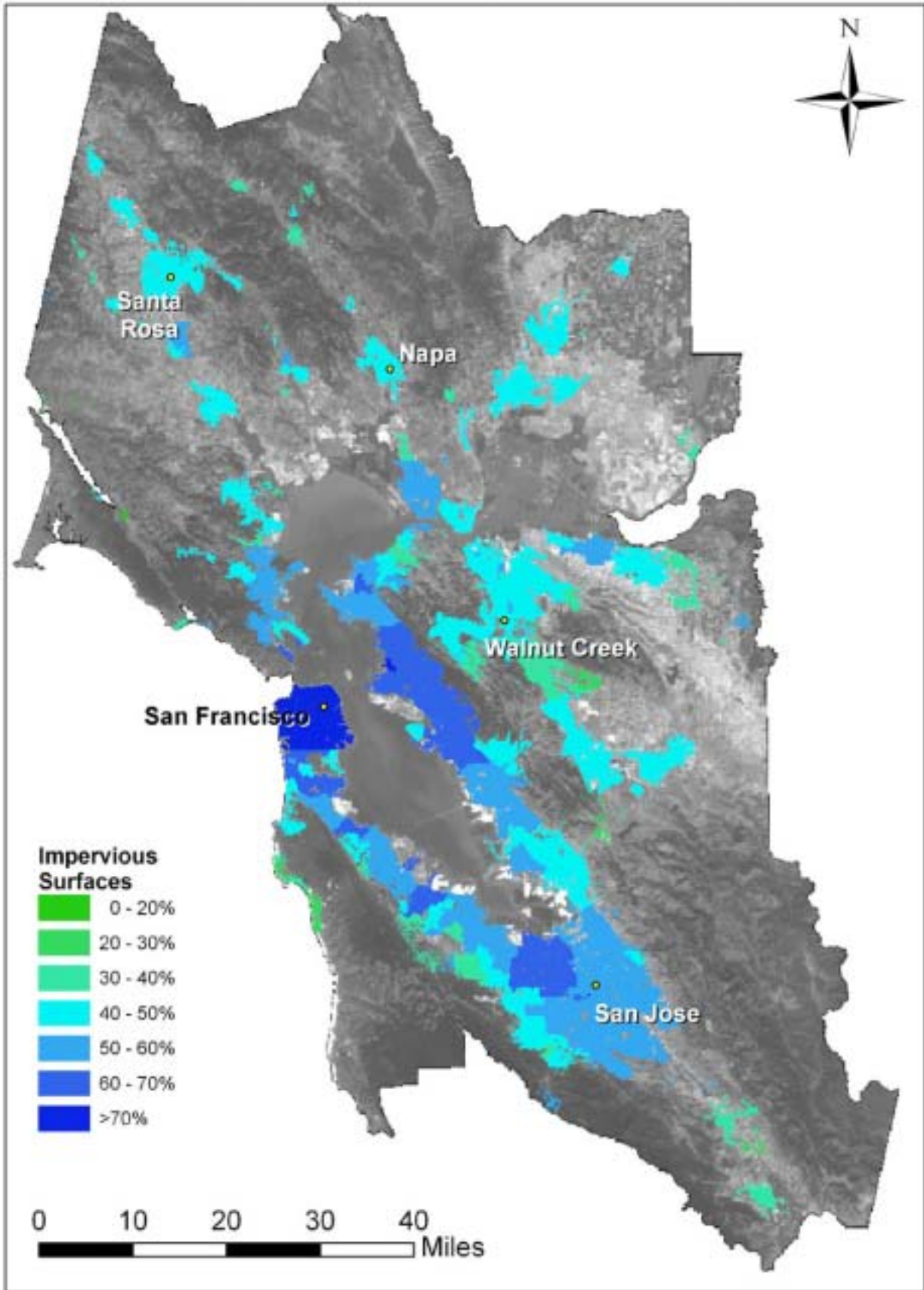


Figure 12. 1995 impervious surface extent for each of the urban areas within the study area.

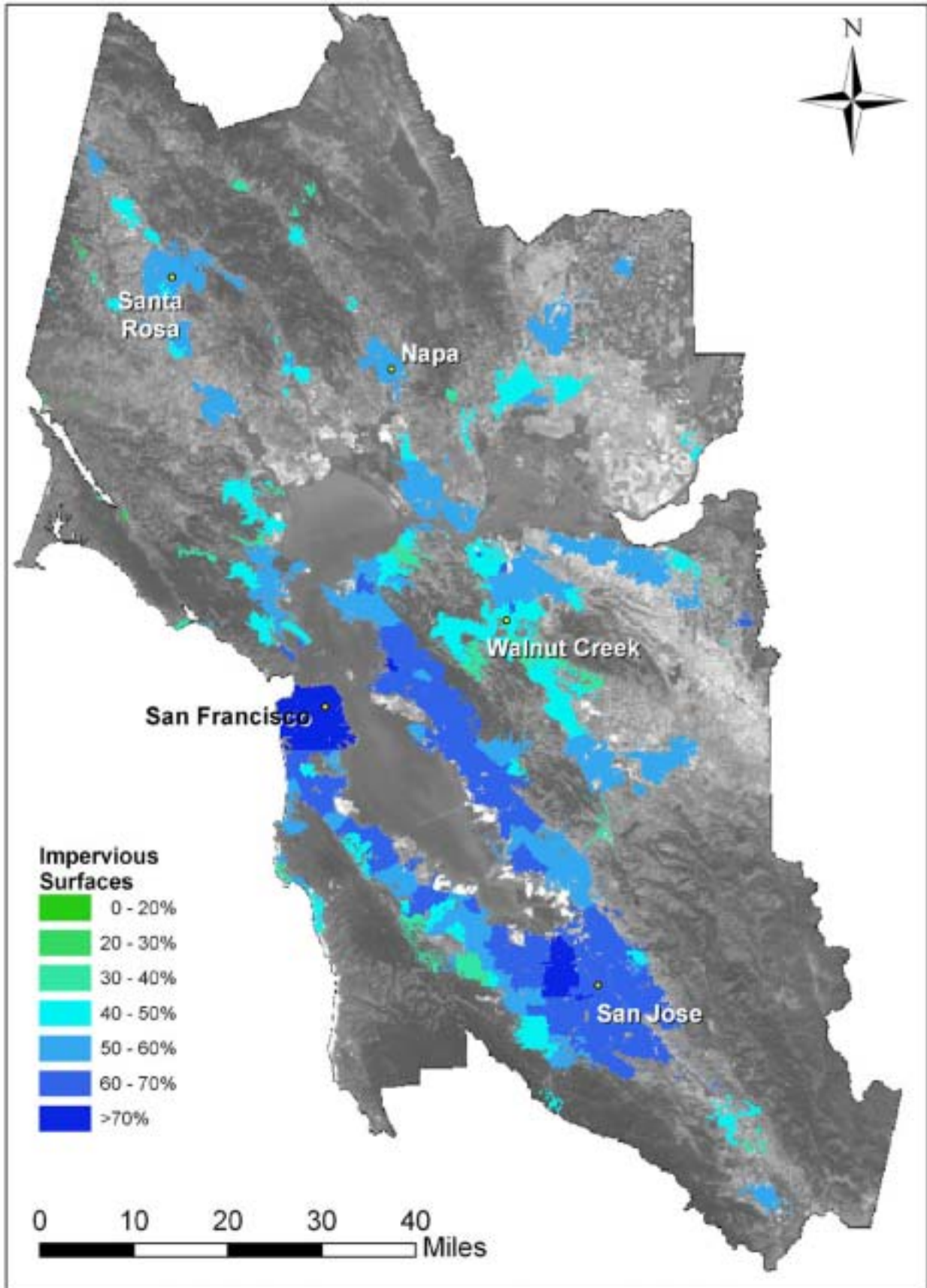


Figure 13. 2002 impervious surface extent for each of the urban areas within the study area.

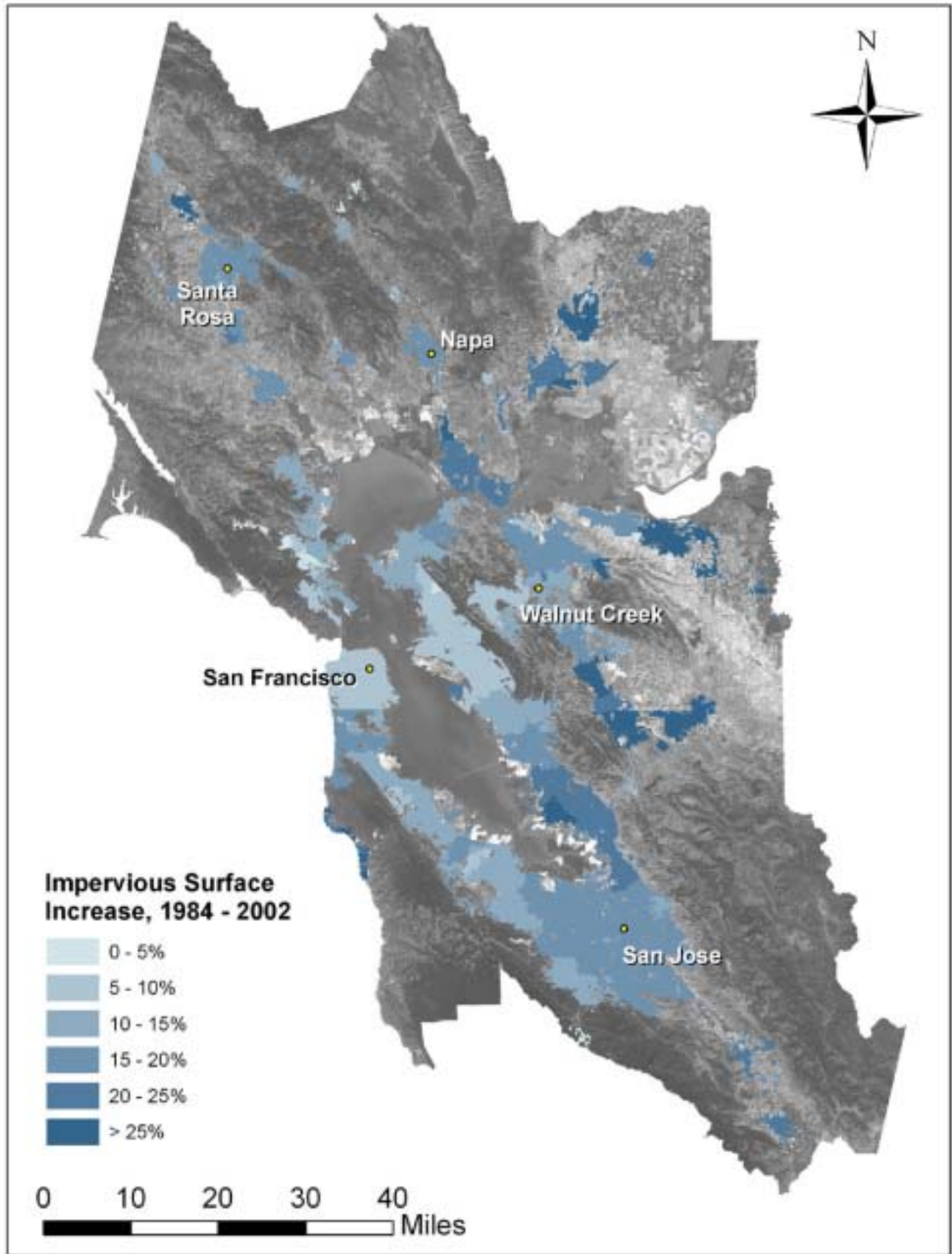


Figure 14. Impervious surface increase from 1984 to 2002 per urbanized area.

The previous figures described how land cover has converted within areas that are currently urbanized. We also studied the pattern and change of overall urban extent for the 1984, 1995, and 2002 time periods. Figure 15 shows the change in urban extent. Urban expansion is primarily around cities not bordering the bay. This includes cities such as Santa Rosa, Fairfield, Pleasanton, Livermore, the Delta Region near Antioch, and Morgan Hill. There has also been expansion south of San Jose but the majority of urban increase near San Jose appears to be from infilling.

The California Department of Forestry (CDF) has also classified urban areas for the San Francisco Bay region (CDF 2002). Figure 16 compares the urban classification of the CDF with the urban classification from the spectral mixture analysis. The CDF urban extent is larger than the SMA urban extent. The CDF urban extent is not limited to the 2000 Census urbanized area boundaries. The CDF urban classification also classifies the wetland surrounding the San Francisco Bay as urban. There are also several examples of agricultural fields and brightly illuminated forest areas that are also classified as urban areas. The SMA urban classification may underestimate urban extent but the CDF urban classification over estimates urban extent.

The USGS has also released the preliminary impervious surface extent for the Bay Area as part of the National Land Cover Dataset (NLCD) 2001 (MRLC 2005). Most areas agree within 10% of the SMA impervious surface measurement with the USGS NLCD 2001 impervious surfaces. Figure 17 shows the SMA impervious surface minus the NLCD 2001 impervious surface. The SMA impervious surface measures a higher impervious surface fraction near forested areas and a lower fraction in agricultural areas

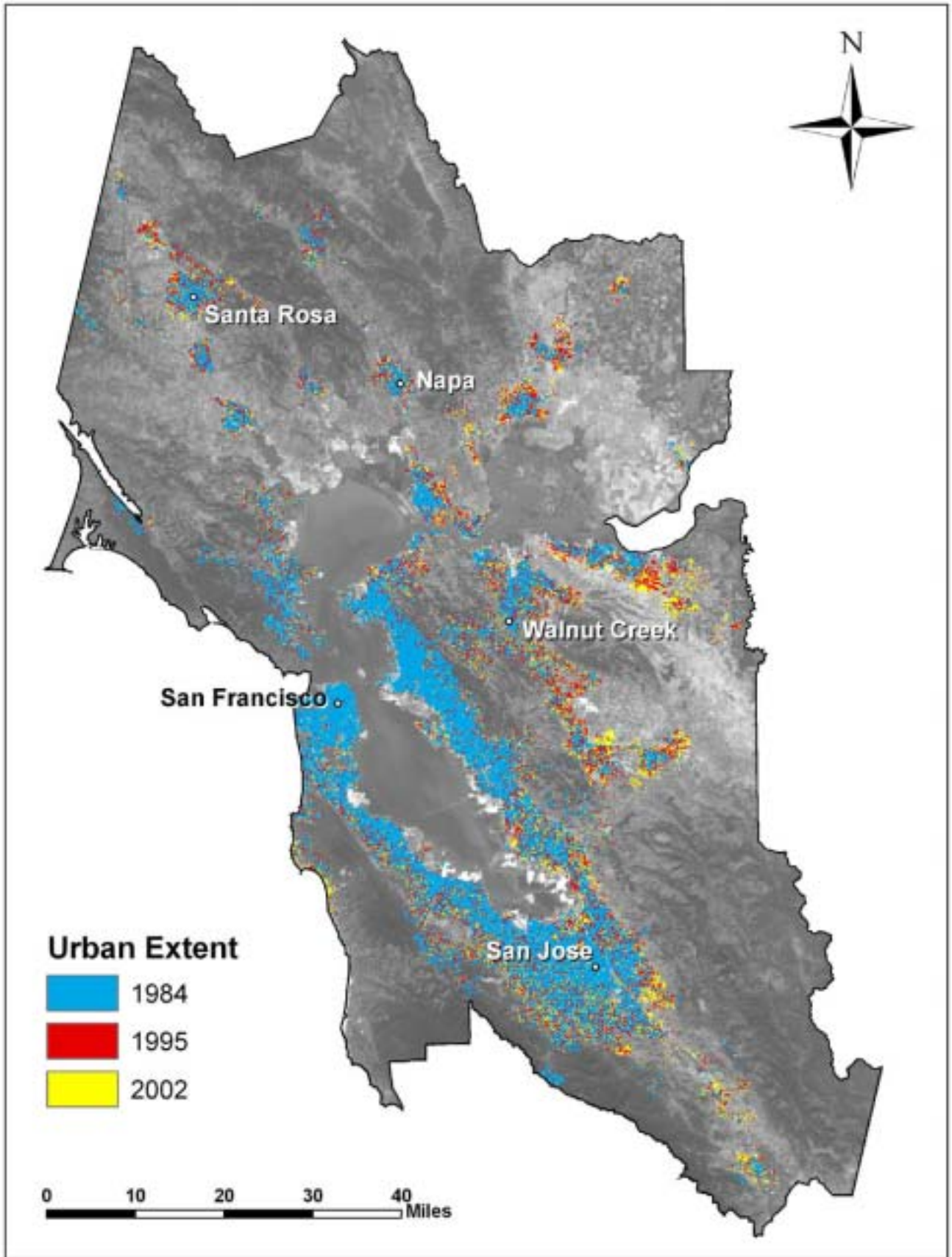


Figure 15. Urban extent for 1984, 1995, and 2002 from SMA urban classification.

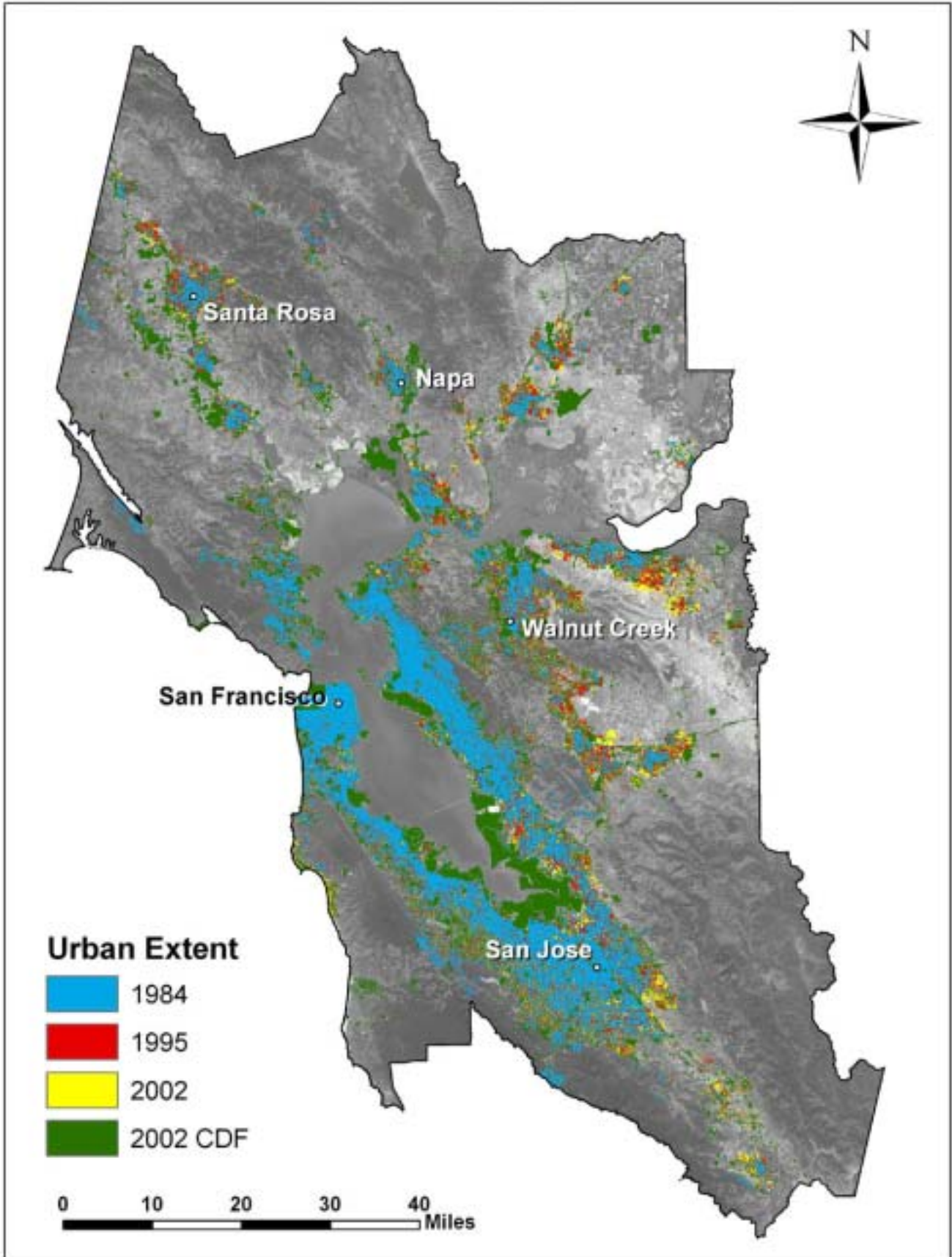


Figure 16. Comparison of urban extent from the SMA classification and CDFs 2002 urban classification.

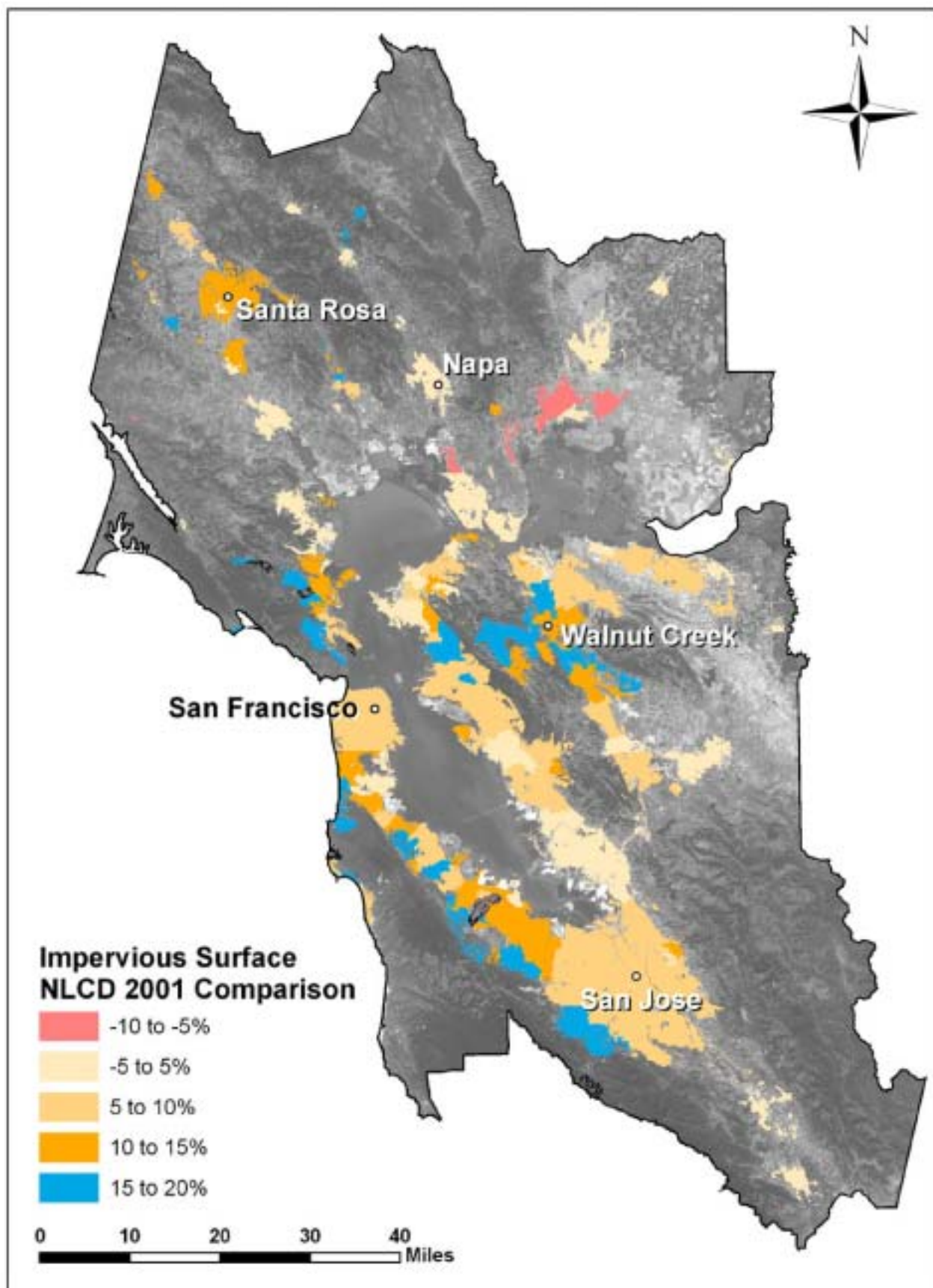


Figure 17. Comparison of impervious surface from the SMA and the 2001 NLCD by urbanized area.

than the NLCD 2001 impervious surface. The areas of disagreement are in areas of more forest cover at the wildland-urban interface. The USGS has not yet determined the error associated with the NLCD 2001 dataset.

Santa Rosa provides a good example of what is happening through out the San Francisco Bay Area (figures 18 - 21). The majority of change is caused by an increase in urban area surrounding the core of the city. The expansion is primarily into rangeland and agricultural land. There is some loss of canopy cover when the urban area expands between 1995 and 2002 into a forested area in the north part of town. This can be seen in figures 18d and 19 where there is a decrease in canopy cover from the building of a residential area (red area of figure 19). The change in canopy cover that is greater or less than the RMS and systematic error for canopy cover is shown in Figure 19.

The majority of the expansion of Santa Rosa occurs between 1984 and 1995. This is seen clearly in figure 13 with the increase of impervious surfaces into areas that were formally agricultural areas. The primary source of change in this area is caused by overall urban expansion. Figure 21 is the change in impervious surface that is greater than the RMS and systematic error from 1984 to 2002

There are other processes that change landcover during this twenty year period besides urban expansion. Canopy cover increases within established urban areas as trees are added and grow larger. Canopy cover is also removed by fire, disease and tree removal. The Tunnel Fire in 1991 in the Oakland Hills provides an example of this (figure 22). In the zoom windows of 1984, 1995, and 2002 (figure 22), the green is

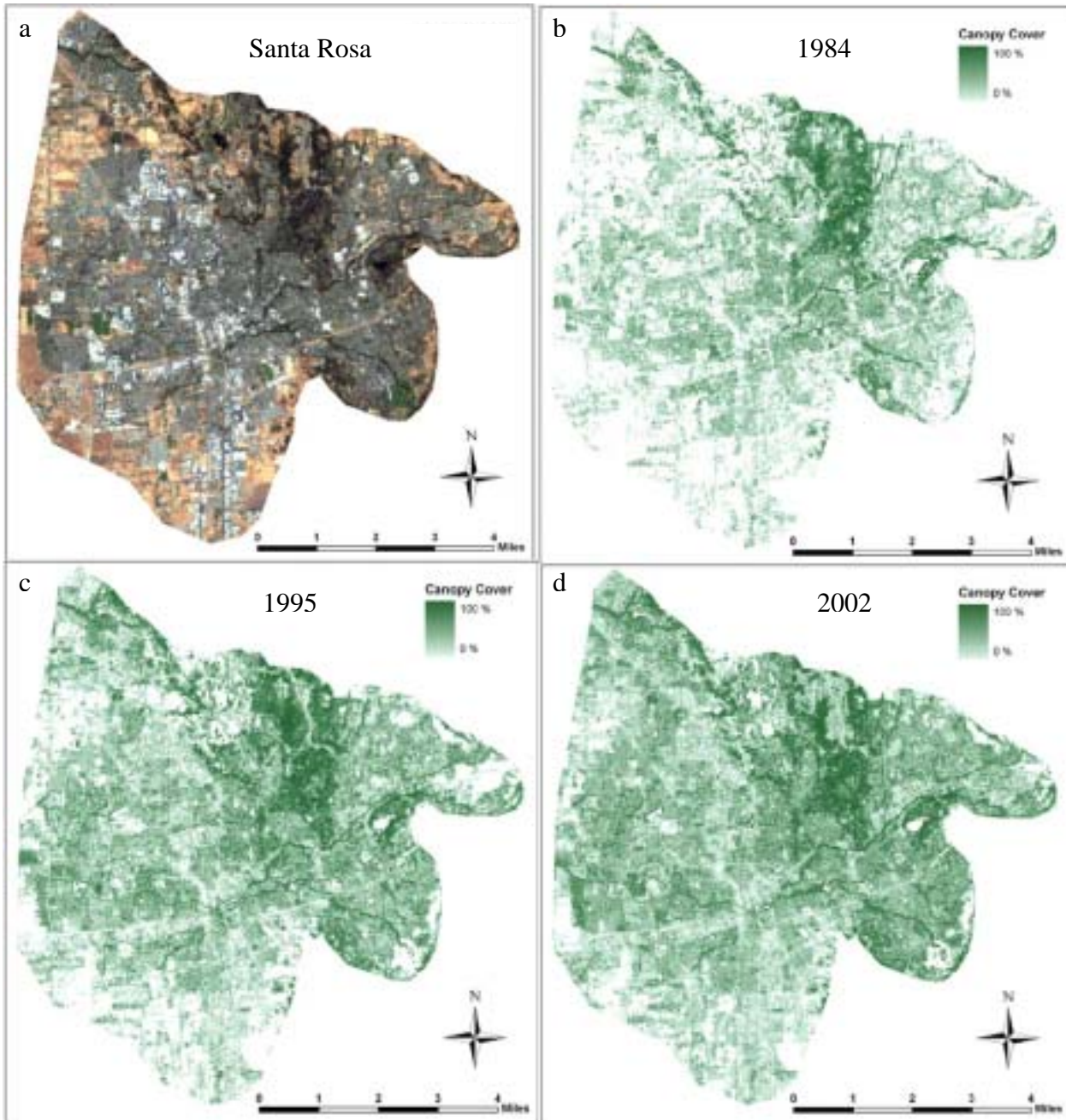


Figure 18. An example of increasing canopy cover with urbanization. The only area where canopy cover decreases is in the north section of town that expands into a forested area in 2002. Figure a is the natural color satellite image of Santa Rosa in 2002.

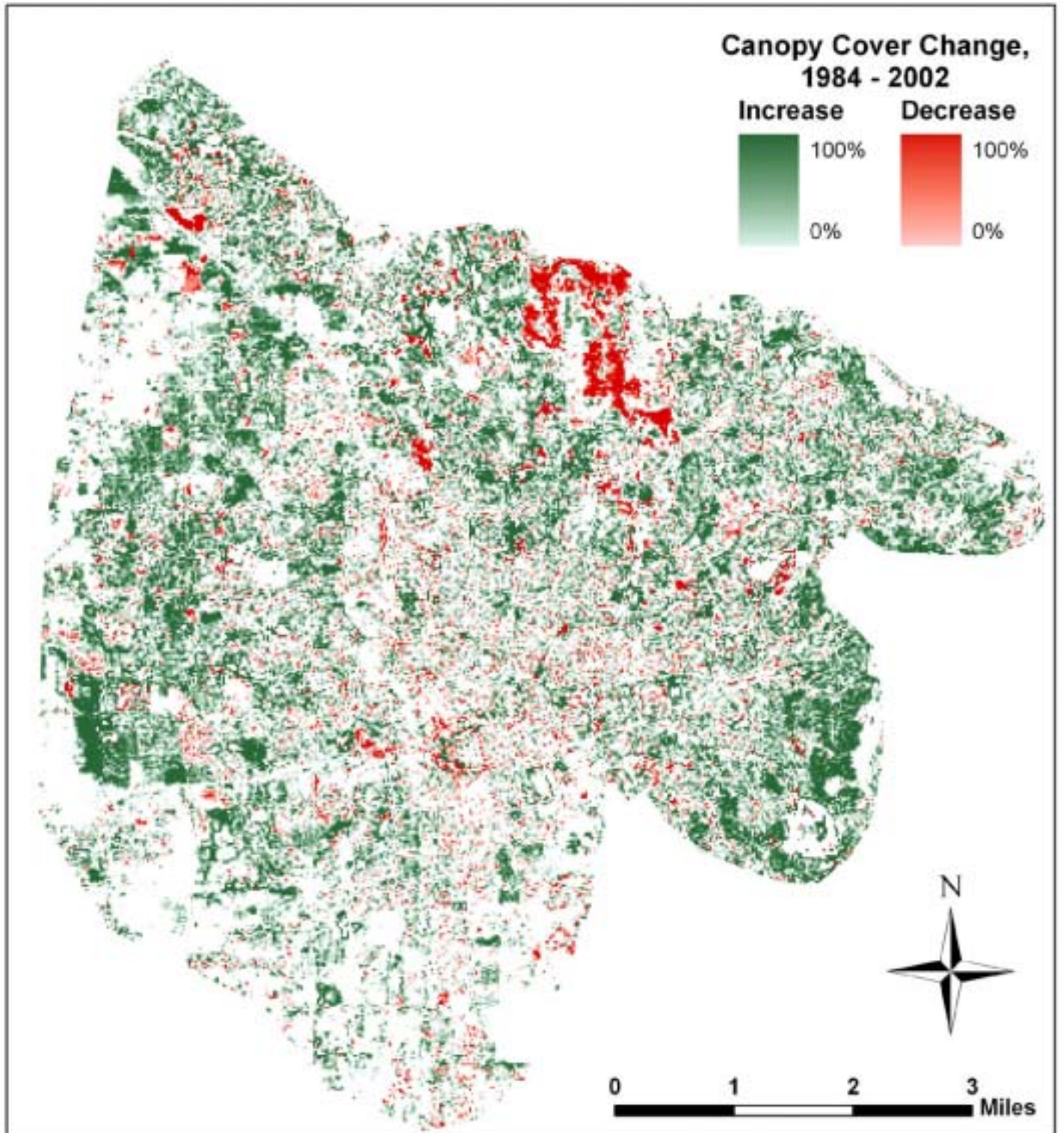


Figure 19. The change in canopy cover that is greater than or less than the associated per-pixel error for canopy cover from 1984 to 2002 in Santa Rosa,.

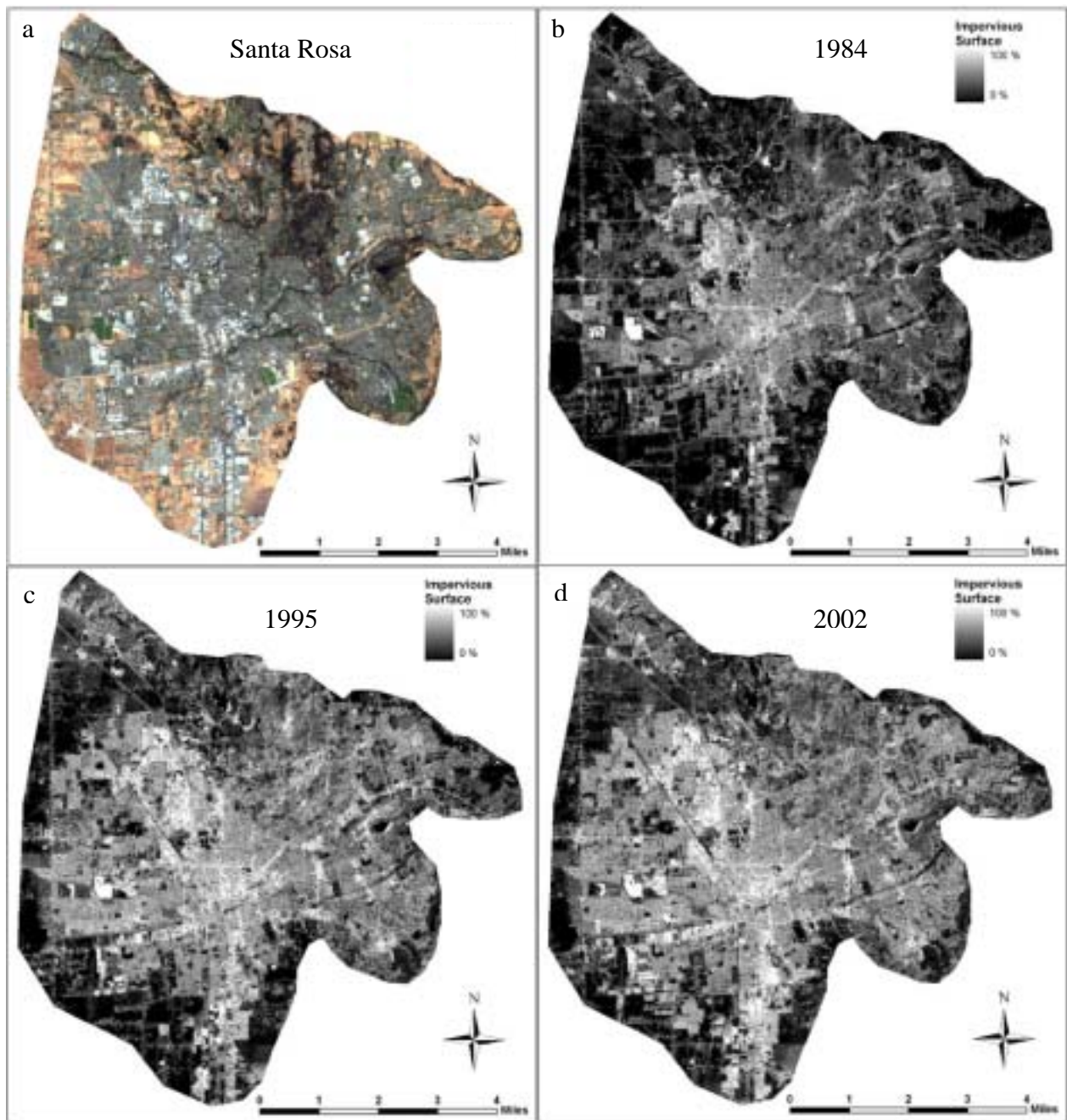


Figure 20. An example of increasing impervious surface with urbanization. Figure a is the natural color satellite image of Santa Rosa in 2002.

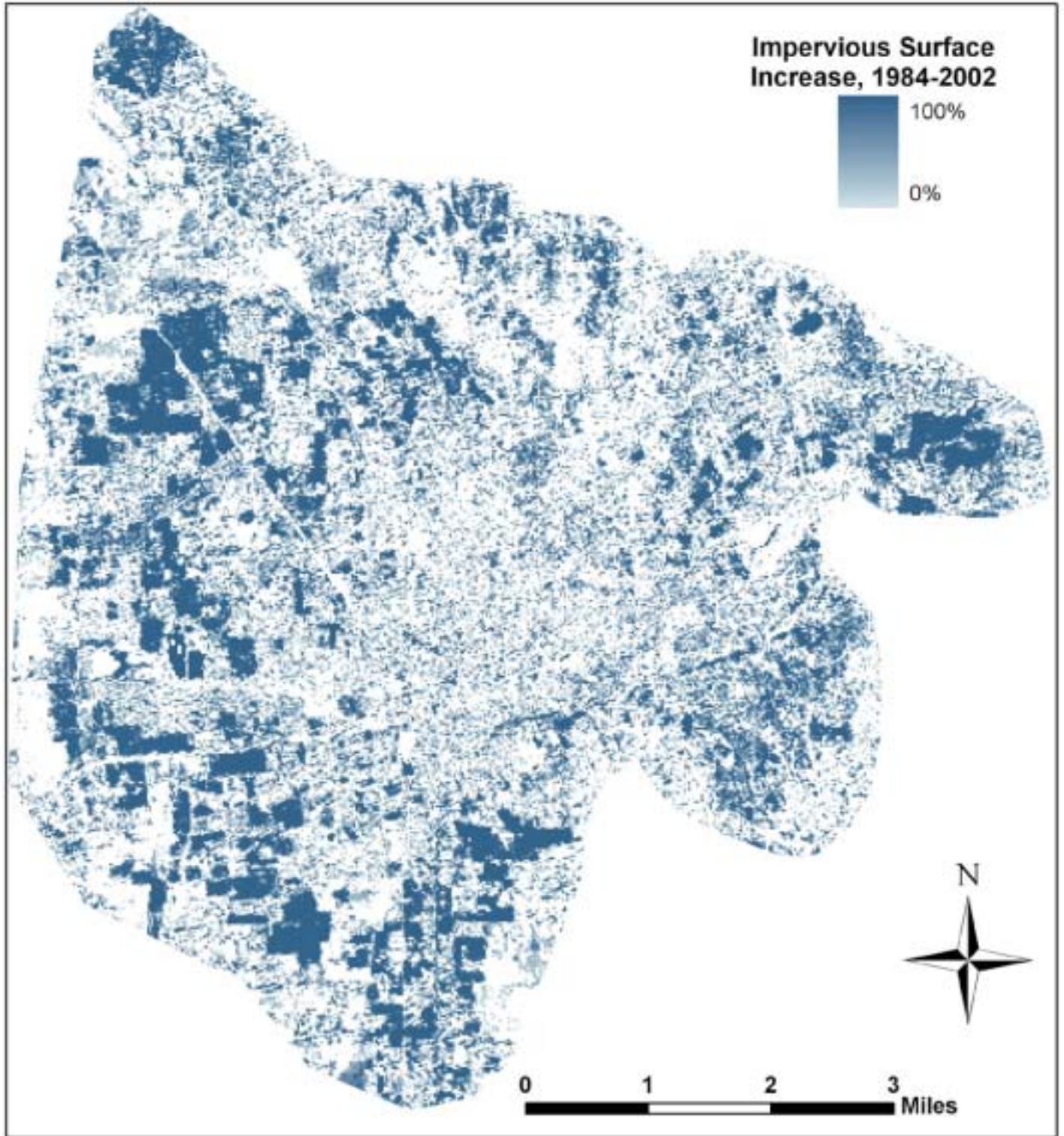


Figure 21. The increase in impervious surface that is greater than the associated per-pixel error for impervious surface from 1984 to 2002 in Santa Rosa,.

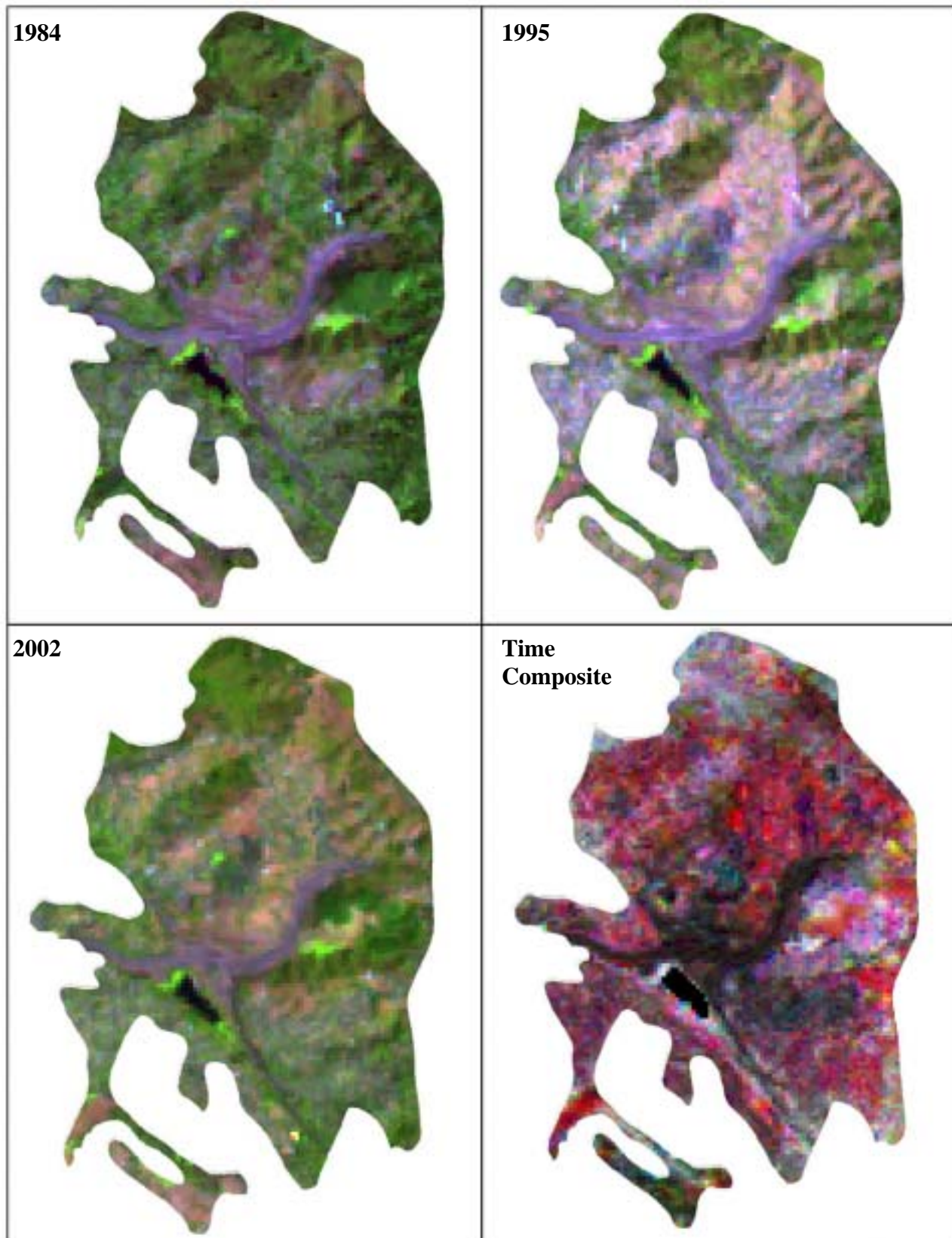


Figure 22. Changes in urban canopy cover from the Tunnel fire in 1991 in the Oakland Hills.

vegetation and canopy cover, tan is exposed ground, blue and grey are impervious surfaces, and the black near the center of the windows is a body of water. The time composite window color codes how the canopy cover changes through this time period. Red is an overall decrease in canopy cover, the magenta are areas where canopy has been fully restored since the fire, and gray and black are areas that have not changed in vegetation. The black area in the time composite corresponds with a road that passes through the center of the image. The areas of magenta, where vegetation has completely returned, correspond with natural occurring vegetation on slopes within the burn. The red areas, where the vegetation has not completely returned, are associated with residential areas.

Conclusions

The urban environment in the San Francisco Bay Area has rapidly expanded into predominately rangeland and agricultural areas. A population increase of 30% has driven a 73% increase in urban area. The increase in urban area is associated with increased canopy cover, but this 10% increase of has not kept pace with the 17% increase in impervious surfaces. This was especially true between 1984 and 1995 when impervious surfaces increased nearly twice as much as canopy cover. With the exception of San Jose, the pattern of urban growth or increase in urban extent has been in areas outside the immediate vicinity of the San Francisco Bay.

The next phase of the project will calculate the benefit and cost per canopy cover area for the entire San Francisco Bay Area.

References

- ABAG. (2003). "Population by Race/Ethnicity and County, 1980-2000." Association of Bay Area Governments. Last Accessed on June 14, 2005, from <http://www.abag.ca.gov/abag/overview/datacenter/popdemo/>.
- CaSIL. (2004). "CalView Landsat Images." The California Spatial Information Library. Last Accessed on June 14, 2005, from <http://casil.ucdavis.edu/casil/gis.ca.gov/landsat7/>.
- CDF. (2002). "Multi-source Land Cover Data (v02_2)." 2002_2. California Department of Forestry and Fire Protection. Last Accessed on June 14, 2005, from http://frap.cdf.ca.gov/projects/frap_veg/index.asp.
- ERDAS (2002). ERDAS Field Guide. Sixth Edition. Atlanta, Georgia, ERDAS.
- Gilabert, M. A., F. J. Garcia-Haro and J. Melia (2000). "A Mixture modeling approach to estimate vegetation parameters for heterogeneous canopies in remote sensing." Remote Sensing of Environment **72**: 328-345.
- Jensen, J. R. (1996). Introductory Digital Image Processing: A Remote Sensing Perspective. Second Edition. Upper Saddle River, New Jersey, Prentice Hall.
- King, J. (2005). Urban centers slow to turn green. San Francisco Chronicle. San Francisco: B1-B2.
- Lu, D. and Q. Weng (2004). "Spectral mixture analysis of the urban landscape in Indianapolis city with Landsat ETM+ imagery." Photogrammetric Engineering & Remote Sensing **70**(9): 1053-1062.
- MRLC. (2005). "2001 National Land Cover Database." Multi-Resolution Land Characteristics Consortium. Last Accessed on June 14, 2005, from <http://www.mrlc.gov/>.
- Phinn, S., M. Stanford, P. Scarth, A. T. Murray and P. T. Shyy (2002). "Monitoring the composition of urban environments based on the vegetation-impervious surface-soil (VIS) model by subpixel analysis techniques." International Journal of Remote Sensing **23**(20): 4131-4153.
- Ridd, M. K. (1995). "Exploring a V-I-S (vegetation-impervious surface-soil) model for urban ecosystem analysis through remote sensing: comparative anatomy for cities." International Journal of Remote Sensing **16**(12): 2165-2185.
- Roberts, D. A., G. T. Batista, J. L. G. Pereira, E. K. Waller and B. W. Nelson (1999). Change identification using multitemporal spectral mixture analysis: Applications in eastern Amazonia. Remote Sensing Change Detection: Environmental Monitoring Methods and Applications R. S. Lunetta and C. D. Elvidge. London, Taylor & Francis: 137-162.

- Small, C. (2001). "Estimation of urban vegetation abundance by spectral mixture analysis." International Journal of Remote Sensing **22**: 1305-1334.
- Small, C. (2002). "Multitemporal analysis of urban reflectance." Remote Sensing of Environment **81**: 427-442.
- Small, C. (2003). "High spatial resolution spectral mixture analysis of urban reflectance." Remote Sensing of Environment **88**: 170-186.
- Small, C. (2004). "The Landsat ETM+ spectral mixing space." Remote Sensing of Environment **93**: 1-17.
- Small, C. (2005). "A global analysis of urban reflectance." International Journal of Remote Sensing **26**(4): 661-681.
- U.S. Census Bureau. (2002). "Census 2000 Urban and Rural Classification." U.S. Census Bureau. Last Accessed on June 14, 2005, from http://www.census.gov/geo/www/ua/ua_2k.html.
- USGS. (2003). "North American Shaded Relief." USGS EROS Data Center. Last Accessed on June 14, 2005, from <http://nationalatlas.gov/atlasftp.html>.
- USGS. (2004). "High Resolution Orthoimagery." USGS EROS Seamless Data Distribution System. Last Accessed on June 16, 2005, from <http://seamless.usgs.gov/>.
- USGS. (2005). "Landsat 7 Calibration Parameter Files." USGS Landsat Program. Last Accessed on June 21, 2005, from <http://landsat.usgs.gov/cpf/default.html>.
- Wu, C. (2004). "Normalized spectral mixture analysis for monitoring urban composition using ETM+ imagery." Remote Sensing of Environment **93**: 480-492.
- Wu, C. and A. T. Murray (2003). "Estimating impervious surface distribution by spectral mixture analysis." Remote Sensing of Environment **84**: 493-505.